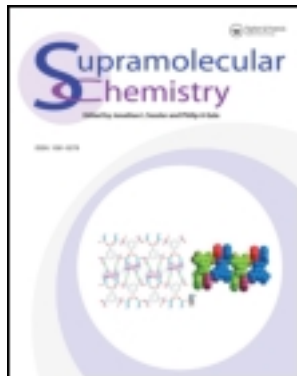


This article was downloaded by: ["Queen's University Libraries, Kingston"]

On: 12 August 2013, At: 20:49

Publisher: Taylor & Francis

Informa Ltd Registered in England and Wales Registered Number: 1072954 Registered office: Mortimer House, 37-41 Mortimer Street, London W1T 3JH, UK



Supramolecular Chemistry

Publication details, including instructions for authors and subscription information:

<http://www.tandfonline.com/loi/gsch20>

A blue-green-emitting 3D supramolecular compound: synthesis, crystal structure and effect of solvents and temperature on the luminescent properties

Xin-Ming Wang^a, Liang-Sheng Qiang^a, Rui-Qing Fan^a, Ping Wang^a & Yu-Lin Yang^a

^a Department of Chemistry, Harbin Institute of Technology, Harbin, 150001, P.R. China

Published online: 07 Jun 2013.

To cite this article: Xin-Ming Wang, Liang-Sheng Qiang, Rui-Qing Fan, Ping Wang & Yu-Lin Yang (2013) A blue-green-emitting 3D supramolecular compound: synthesis, crystal structure and effect of solvents and temperature on the luminescent properties, *Supramolecular Chemistry*, 25:7, 416-423, DOI: [10.1080/10610278.2013.792340](https://doi.org/10.1080/10610278.2013.792340)

To link to this article: <http://dx.doi.org/10.1080/10610278.2013.792340>

PLEASE SCROLL DOWN FOR ARTICLE

Taylor & Francis makes every effort to ensure the accuracy of all the information (the "Content") contained in the publications on our platform. However, Taylor & Francis, our agents, and our licensors make no representations or warranties whatsoever as to the accuracy, completeness, or suitability for any purpose of the Content. Any opinions and views expressed in this publication are the opinions and views of the authors, and are not the views of or endorsed by Taylor & Francis. The accuracy of the Content should not be relied upon and should be independently verified with primary sources of information. Taylor and Francis shall not be liable for any losses, actions, claims, proceedings, demands, costs, expenses, damages, and other liabilities whatsoever or howsoever caused arising directly or indirectly in connection with, in relation to or arising out of the use of the Content.

This article may be used for research, teaching, and private study purposes. Any substantial or systematic reproduction, redistribution, reselling, loan, sub-licensing, systematic supply, or distribution in any form to anyone is expressly forbidden. Terms & Conditions of access and use can be found at <http://www.tandfonline.com/page/terms-and-conditions>

A blue-green-emitting 3D supramolecular compound: synthesis, crystal structure and effect of solvents and temperature on the luminescent properties

Xin-Ming Wang, Liang-Sheng Qiang, Rui-Qing Fan*, Ping Wang and Yu-Lin Yang

Department of Chemistry, Harbin Institute of Technology, Harbin 150001, P.R. China

(Received 11 January 2013; final version received 29 March 2013)

A blue-green-emitting three-dimensional supramolecular compound ($C_{10}O_2N_2H_8$)($C_9O_7H_6$) (**1**) was synthesised under hydrothermal conditions and structurally characterised by elemental analysis, IR spectrum, 1H NMR and single-crystal X-ray diffraction. The crystal belongs to triclinic system with $P\bar{1}$ space group. The crystal structure is stabilised by $O-H\cdots O$, $O-H\cdots N$ hydrogen bonds and $\pi-\pi$ interactions ($\pi-\pi$ stacking distance is 3.282 Å). Compound **1** exhibits intense green luminescence in solid state at 298 K ($\lambda_{em} = 546$ nm). In addition, absorption and fluorescence characteristics of compound **1** have been investigated in different solvents (DMSO, CH_3CN and CH_3OH). The results show that compound **1** exhibits a large red shift in both absorption and emission spectra as solvent polarity increases (polarity: $DMSO > CH_3CN > CH_3OH$), indicating a change in dipole moment of compound **1** upon excitation. Although the emission spectra of compound **1** in CH_3OH are close to it in dimethyl sulfoxide (DMSO), it is revealed that the luminescence behaviour of compound **1** depends not only on the polarity of environment but also on the hydrogen bonding properties of the solvent. Meanwhile, temperature strongly affects the emission spectra of compound **1**. Emission peaks of compound **1** were blue shift at 77 K than those at 298 K in both solid state (*ca.* 142 nm) and solution (*ca.* 6–23 nm), which was due to the non-radiative transition decreases at low temperature. Moreover, the quantum yield and fluorescence lifetime of compound **1** were also measured, which increased with increasing polarity of solvent, lifetime in DMSO at 298 K ($\tau_1 = 0.92$ μs , $\tau_2 = 8.71$ μs) was the longest one in solvents (298 K: $\tau_1 = 0.87$ – 0.92 μs , $\tau_2 = 7.50$ – 8.71 μs ; 77 K: $\tau_1 = 0.72$ – 0.90 μs , $\tau_2 = 6.88$ – 7.45 μs), which was also shorter than that in solid state (298 K: $\tau_1 = 1.13$ μs , $\tau_2 = 7.50$ μs ; 77 K: $\tau_1 = 0.97$ μs , $\tau_2 = 8.97$ μs). This was probably because of the weak polarity environment of compound **1** in solid state.

Keywords: supramolecular compound; hydrogen bonds; fluorescence characteristics in different solvents; quantum yield

1. Introduction

Various non-covalent weak interactions play significant roles in supramolecular architecture. In crystal engineering (1) and supramolecular chemistry (2), hydrogen bonding system (3), as well as various non-bonding weak interactions (4) such as $\pi-\pi$ stacking interactions, is the main key for the organisation of self-assembling supramolecule. In molecular recognition, hydrogen bond ($O-H\cdots O$, $O-H\cdots N$ and $N-H\cdots O$) is the most important interaction because of its strength and directional properties (5). Aromatic $\pi-\pi$ stacking interactions are all pervasive in nature in molecular level; they play important roles in the stacking of supramolecule (6). In addition, some crystals of organic small molecules not only have potential advantages in lower synthetic costs but also possess organic light emitting properties (7, 8). The compounds with $\pi-\pi$ stacking interactions mostly have aromatic structures, and could take place $\pi-\pi^*$ (9, 10) or $n-\pi^*$ (11) transitions which are responsible for most of the optical processes. Many novel complexes with non-covalent interactions have attracted considerable

attention due to their potential application in materials with luminescent and nonlinear optical properties (12–16).

In this study, we designed and synthesised the supramolecular compound **1** which possesses green emission in solid state. Compound **1** consists of a 2-hydroxyl-1,3,5-tricarboxylic acid (H_4OTBA) and a 4-(1H-Imidazol-1-yl) benzoic acid (HIBA), which are connected by hydrogen bonds. As other organic acid–base compounds, HIBA is an aromatic carboxylic acid and *N*-containing compound. What is a fascinating and unique feature of HIBA is that its structure contains imidazole ring and benzene ring which are linked by a C–N single bond. Imidazole and its derivatives exhibit a broad spectrum of biological and biochemical activity, processes occurring in living systems have been attributed to them (17). Imidazoles have been applied as a chromophore with tunable absorption wavelength (18). They also attract special attention of the researchers who work on metal–organic frameworks and organic molecular crystals in recent years (19–21). The aromatic rings of HIBA could make $\pi-\pi$ stacking possible, as well as hydrogen bonds,

*Corresponding author. Email: fanruiqing@hit.edu.cn

and build a steady supramolecular structure (22, 23). In addition, in order to study the effects of surrounding environment on different fluorescence properties (e.g. maximum emission wavelength, fluorescence quantum yield and fluorescence lifetime) of compound **1**, we recorded the fluorescence spectra and fluorescence decay curves of compound **1** in solid state and solutions (DMSO, CH₃CN and CH₃OH) at 298 and 77 K, the relevance of environment to luminescent properties of compound **1** is discussed in detail.

2. Experimental

2.1. General characterisation

All solvents and reagents were of analytical reagent grade. Elemental analyses (C, H and N) were performed on a Perkin-Elmer 240c elemental analyser. IR spectra were recorded by Nicolet Impact 410 FTIR spectrometer (KBr pellets, range in 4000–400 cm⁻¹). ¹H NMR (400 MHz) spectra were recorded on a Bruker ACF 400 MHz at room temperature (rt). (UV–vis spectra were obtained on a Perkin-Elmer Lambda 20 spectrometer. Photoluminescence analysis and fluorescence decay curves were recorded on Edinburgh FLS920 fluorescence spectrometer at 298 and 77 K.

2.2. Synthesis of compound (C₁₀O₂N₂H₈)(C₉O₇H₆) (**1**)

A mixture of 2-hydroxyl-1,3,5-tricarboxylic acid (H₄OTBA) (0.0226 g), HIBA (0.0188 g), with a molar ratio of 1:1 was mixed in the distilled water (5 mL). After stirring for 1 h in air, it was transferred into a 15 mL Teflon-lined stainless steel autoclave and heated at 160°C for 4 days. After cooling to the rt, the mixture was washed with distilled water, filtered off and dried, then yellow block crystals were obtained in a 54% yield, based on H₄OTBA. The resultant crystal was stable in air and insoluble in water or common organic solvents such as dichloromethane, toluene and tetrahydrofuran (THF). IR bands (KBr pellet, cm⁻¹): 3448 s, 3137 w, 1608 m, 1525 m, 1413 s, 1305 m. Anal. calcd for compound **1** (%): C, 55.08; H, 3.40; N, 6.76. Found: C, 55.24; H, 3.57; N, 6.60.

2.3. X-ray diffraction analysis

Suitable crystals of compound **1** were mounted on glass fibres for single-crystal X-ray measurement. Reflection data were collected on a Siemens SMART 1000 CCD diffractometer equipped with graphite-monochromated Mo K α radiation ($\lambda = 0.71073 \text{ \AA}$), operating at $298 \pm 2 \text{ K}$. The structure was solved by direct method and refined by full-matrix least squares based on F^2 using the SHELXTL 5.1 software package (24). The hydrogen atoms were placed at calculated positions and refined as

riding atoms with isotropic displacement parameters. All non-hydrogen atoms were refined anisotropically. Crystallographic data for compound **1** are given in Table 1, and selected bond lengths and bond angles are listed in Table S1 of the Supplementary Information, available online. Cambridge Crystallographic Data Centre as supplementary publication No. CCDC-918773. Copies of the data can be obtained free of charge on application to CCDC, 12 Union Road, Cambridge CB2 1EZ, UK (fax: +44 1223/336 033; deposit@ccdc.cam.ac.uk).

3. Results and discussion

3.1. Structure description

The result of single-crystal X-ray diffraction analysis revealed that compound **1** is triclinic and crystallises in a space group. The asymmetric unit contains one H₄OTBA and one HIBA molecule, which is shown in Figure 1. The supramolecular structure of compound **1** was established by asymmetric unit through non-covalent intermolecular and intramolecular interactions including hydrogen bonding and π – π stacking interactions (the parameters of hydrogen bonds are given in Table 2), the crystal packing structure of compound **1** is shown in Figure 2.

This conformation is stabilised by intramolecular/intermolecular hydrogen bonding and π – π stacking interactions. In compound **1**, following ones can be found: O–H \cdots O, O–H \cdots N, and donor \cdots acceptor distance is in the range of 3.055–2.639 Å. The shortest distance 2.639 Å refers to the intramolecular O9–H9 \cdots O8 ($\angle\text{OHO} = 166.63^\circ$) hydrogen bond. For HIBA molecule, the conjugated imidazole ring and benzene ring are not co-planar but with a dihedral angle about 40° . The angle that carboxyl deviated from benzene ring of HIBA molecule is 6.79° . For H₄OTBA molecule, O1–H1 \cdots O2 ($\angle\text{OHO} = 139.48^\circ$) and O2–H2 \cdots O1 ($\angle\text{OHO} = 141.80^\circ$) intramolecular hydrogen bonds lead to deviations of the carboxyls from benzene ring average plane: 1-carboxylate group deviates by 15.96° , 3-carboxylate group by 59.79° and 5-carboxylate group by 2.06° . The hydroxyl group and its corresponding benzene ring are almost coplanar with the deviation is only about 0.093 Å. There is a significant intermolecular hydrogen bond interaction O2–H2 \cdots N2 in solid state of compound **1**, its bond length is 3.055 Å ($\angle\text{OHN} = 139.58^\circ$). The π – π stacking distance between imidazole ring and benzene ring is 3.282 Å. These two ring planes are not parallel-displaced geometry with the dihedral angle is 10.14° .

3.2. IR spectra of **1**

The IR spectrum of compound **1** is shown in Figure S1 of the Supplementary Information, available online. In the IR spectrum, the absorption bands centred at 3448 cm^{-1} may be assigned to the stretching vibrations of phenolic

Table 1. Crystal data and structure refinement parameters of compound **1**.

Empirical formula	C ₁₉ H ₁₄ N ₂ O ₉
Formula weight	414.32
<i>T</i> (K)	293(2)
Crystal system	Triclinic
Space group	P $\bar{1}$
<i>a</i> (Å)	8.0830(16)
<i>b</i> (Å)	9.6180(19)
<i>c</i> (Å)	11.538(2)
α (°)	91.14(3)
β (°)	101.74(3)
γ (°)	98.74(3)
<i>V</i> (Å ³)	866.8(3)
<i>Z</i>	2
<i>D</i> (Mg m ⁻³)	1.587
μ (mm ⁻¹)	0.129
<i>F</i> (000)	428
Crystal size (mm)	0.50 × 0.30 × 0.19
θ Ranges (°)	3.10–25.00
Max. and min. transmission	0.9758 and 0.9383
Limiting indices	–9 ≤ <i>h</i> ≤ 9 –11 ≤ <i>k</i> ≤ 11 –13 ≤ <i>l</i> ≤ 13
Reflections collected/unique	6865/3043 (<i>R</i> (int) = 0.0241)
Data/restraints/parameters	3043/2/271
Refinement method	Full-matrix least squares on <i>F</i> ²
GOF	1.101
Final <i>R</i> indices (<i>I</i> > 2 σ (<i>I</i>))	<i>R</i> ₁ ^a = 0.0779, <i>wR</i> ₂ ^b = 0.2384
<i>R</i> indices (all data)	<i>R</i> ₁ ^a = 0.0914, <i>wR</i> ₂ ^b = 0.2506
Largest diff. peak and hole (e · Å ⁻³)	0.736 and –0.637

$$^a R_1 = \frac{\sum ||F_o| - |F_c||}{\sum |F_o|}$$

$$^b wR_2 = \left(\frac{\sum (w(F_o^2 - F_c^2))^2}{\sum (w(F_o^2))^2} \right)^{1/2}$$

hydroxyl. The band at 3137 cm⁻¹ is associated with the benzene ring stretching vibrations. The splitting absorption bands at 1608(s) cm⁻¹, 1525(s) cm⁻¹, 1413(s) cm⁻¹ and 1305(s) cm⁻¹ are attributed to carboxylate group asymmetric stretching vibrations (ν_{as}) and symmetric

stretching vibrations (ν_s), respectively (25). Characteristic bands of carboxyl unit appear at 1720–1690 cm⁻¹ (26), whereas the stretching bands of carboxyl groups in compound **1** shift towards lower frequencies and their intensity are slightly reduced, which indicate that there exit

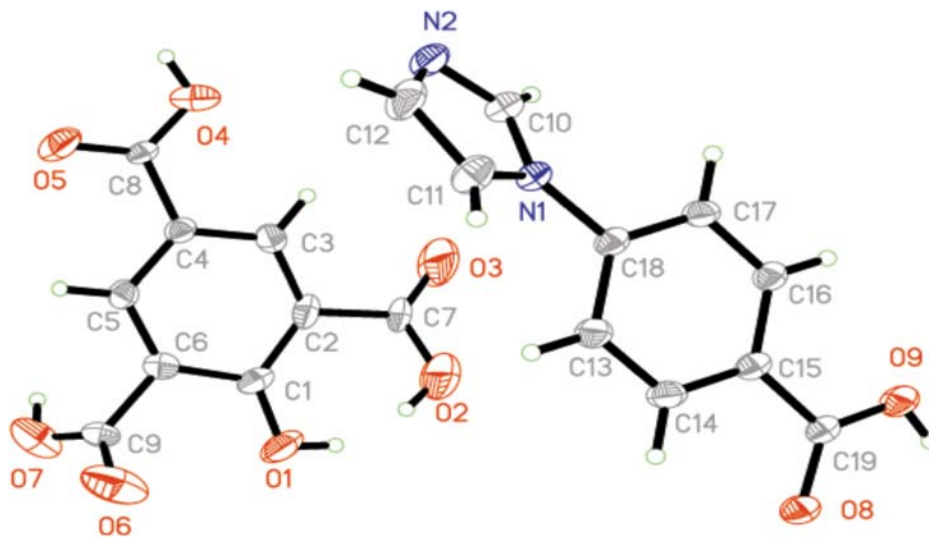
Figure 1. Crystal structure of compound **1**.

Table 2. Important hydrogen bond interactions in compound **1**.

D—H...A	D—H (Å)	H...A (Å)	D...A (Å)	∠D—H...A (°)
O1—H1...O2	0.820(1)	1.989(1)	2.666(1)	139.48(1)
O2—H2...O1	0.820(1)	1.973(1)	2.666(1)	141.80(1)
O2—H2...N2	0.820(1)	2.384(1)	3.055(1)	139.58(1)
O9—H9...O8	0.820(1)	1.835(1)	2.639(1)	166.63(1)

intermolecular or intramolecular hydrogen bond interactions in solid state. This kind of non-covalent bond could inhibit the molecular vibration (27), this was further confirmed by single-crystal X-ray diffraction analysis.

3.3. ^1H NMR spectra

In order to explain the structure of compound **1** in three polar solvents (DMSO, CH_3CN and CH_3OH), ^1H NMR experiments of compound **1** were carried out in $\text{DMSO}-d_6$, $\text{CH}_3\text{CN}-d_3$ and $\text{CH}_3\text{OH}-d_4$, respectively (Figures S2–S4 of the Supplementary Information, available online). ^1H NMR ($\text{DMSO}-d_6$, 400 MHz) δ (ppm) data of compound **1** are 5.00 (s, 1H, $\text{H}_4\text{OTBA}-\text{H}_2$), 7.23 (s, 1H, $\text{HIBA}-\text{H}_{10}$), 7.83–7.85 (t, 3H, $\text{HIBA}-\text{H}_{3,5,11}$), 7.93 (s, 1H, $\text{HIBA}-\text{H}_8$), 8.05–8.08 (t, 2H, $\text{HIBA}-\text{H}_{2,6}$), 8.53 (t, 2H, $\text{H}_4\text{OTBA}-\text{H}_{4,6}$), 8.60 (s, 1H, $\text{HIBA}-\text{COOH}$), 10.70 (m, 3H, $\text{H}_4\text{OTBA}-\text{COOH}$). ^1H NMR ($\text{CH}_3\text{CN}-d_3$, 400 MHz) δ (ppm) data of compound **1** are 4.76 (s, 1H, $\text{H}_4\text{OTBA}-\text{H}_2$), 7.58 (s, 1H, $\text{HIBA}-\text{H}_{10}$), 7.69 (m, 3H, $\text{HIBA}-\text{H}_{3,5,11}$),

7.80 (s, 1H, $\text{HIBA}-\text{H}_8$), 8.17 (m, 2H, $\text{HIBA}-\text{H}_{2,6}$), 8.63–8.64 (d, 2H, $\text{H}_4\text{OTBA}-\text{H}_{4,6}$), 8.93 (s, 1H, $\text{HIBA}-\text{COOH}$), 10.49 (m, 3H, $\text{H}_4\text{OTBA}-\text{COOH}$). ^1H NMR ($\text{CH}_3\text{OH}-d_4$, 400 MHz) δ (ppm) data of compound **1** are 4.93 (s, 1H, $\text{H}_4\text{OTBA}-\text{H}_2$), 7.74 (s, 1H, $\text{HIBA}-\text{H}_{10}$), 7.84–7.87 (t, 3H, $\text{HIBA}-\text{H}_{3,5,11}$), 8.08 (s, 1H, $\text{HIBA}-\text{H}_8$), 8.25–8.26 (t, 2H, $\text{HIBA}-\text{H}_{2,6}$), 8.75–8.76 (t, 2H, $\text{H}_4\text{OTBA}-\text{H}_{4,6}$), 8.94 (s, 1H, $\text{HIBA}-\text{COOH}$), 10.95 (m, 3H, $\text{H}_4\text{OTBA}-\text{COOH}$). In the three ^1H NMR spectra of compound **1**, signals of compound **1** are uniform on the whole. Especially the characteristic peak positions of $\text{H}_4\text{OTBA}-\text{COOH}$ in $\text{DMSO}-d_6$, $\text{CH}_3\text{CN}-d_3$ and $\text{CH}_3\text{OH}-d_4$ are almost the same. ^1H NMR data indicate that compound **1** keeps the same structure in DMSO, CH_3CN and CH_3OH solution.

3.4. Spectral behaviour of **1** in different solvents

3.4.1. UV-vis absorption spectra

In UV-vis spectra, the bands in the wavelength range 230–270 nm could be assigned to the excitation of π -electrons of aromatic system. These bands are sensitive to substitution at aromatic rings and their positions are influenced by changing the solvent polarity (28).

Effects of solvent polarity on the electronic absorption of compound **1** were studied in three organic polar solvents (polarity: $\text{DMSO} > \text{CH}_3\text{CN} > \text{CH}_3\text{OH}$) at 298 K because compound **1** is insoluble in water or common organic solvents. The absorption spectral characteristics of compound **1** are shown in Figure 3. The absorption maximum of compound **1** is observed to shift from 229 to 269 nm with an increase in the solvent polarity from CH_3CN to DMSO, corresponding to $\pi \rightarrow \pi^*$ electronic transition of the aromatic rings (29). The red shift implies that the value of dipole moment is higher in the excited-state structure than it in ground state (30), so the excited state is more sensitive than ground state. With the

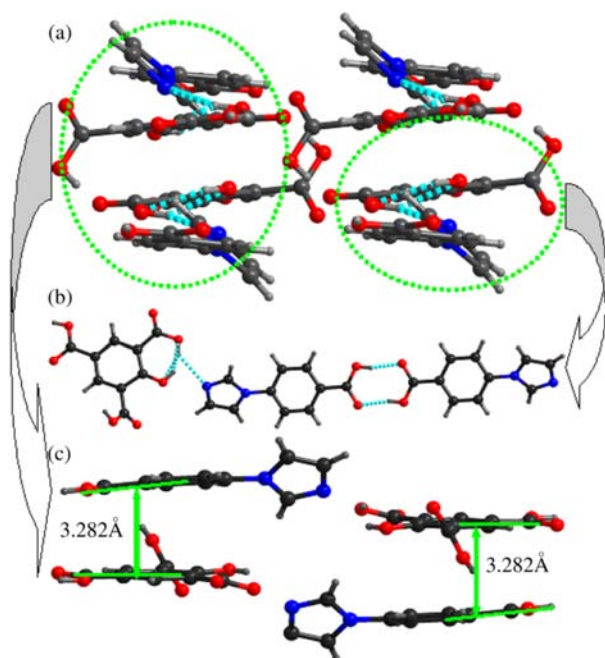


Figure 2. (a) Supramolecular structure of compound **1**, (b) hydrogen bonding interactions between the molecules and (c) packing structure for compound **1**.

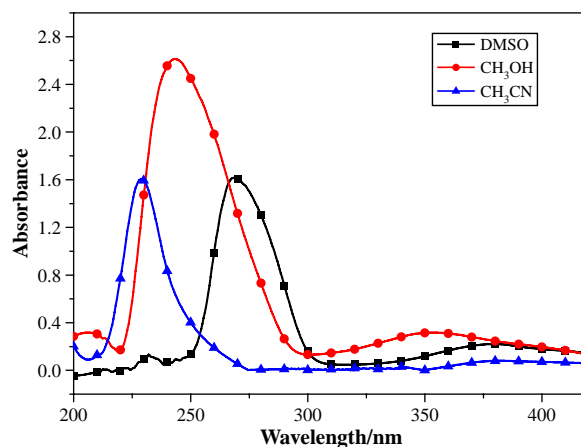


Figure 3. The UV-vis spectra of compound **1** in DMSO, CH_3OH and CH_3CN solutions at 298 K.

increasing of solvents polarity, excited state π^* is to be more stable than ground state π . Thus on going to more polar solvents, the excited state is to be lower energy level, which reduced the energy difference between ground state and excited state, so the absorption spectra are red shift with the increase of solvent polarity.

However, it is important to note that although CH_3CN possesses a more strong polarity than CH_3OH , the UV absorption spectra in CH_3OH ($\lambda = 243$ nm) are red shift than that in CH_3CN ($\lambda = 229$ nm). It may be due to that in polar solvent, the donor ability of hydrogen bond is responsible for a contributing factor for higher extent of stabilisation of excited state (31). CH_3OH is polar protic solvent, which is a hydrogen bond donor with strong polarity; it has very strong interaction with solute through hydrogen bond. CH_3CN is polar aprotic solvent; this kind of solvent cannot be used as a hydrogen bond donor (32). As a result, there has been a red shift to longer wavelength in CH_3OH than in CH_3CN .

3.4.2. Fluorescence spectra

To investigate interaction between the compound molecule and solvent, the emission spectra of compound **1** in solutions (CH_3OH , CH_3CN and DMSO) with the same concentration (1.0×10^{-5} mol/L) were examined by fluorescence spectrophotometry at 298 and 77 K, the results are shown in Figure 4. It is shown that compound **1** displays blue-violet fluorescence emission in these polar aprotic or polar protic solvents in the 400–600 nm region. The emission peaks positions are sensitive to the polarity of medium. Ongoing from CH_3CN to DMSO, low-energy bands of the emission bands of compound **1** are at ca. 476–483 nm, and high-energy emission bands are at ca. 428–447 nm, which can be attributed to $\pi^* \rightarrow \pi$ fluorescence emission (33). It undergoes a red shift (ca. 19 nm) with increasing the solvent polarity from CH_3CN to DMSO, which is attributed to that the ground-state energy distribution is not affected to a greater extent possibly due to the less polar nature than that in excited state. Although DMSO possesses a more strong polarity than CH_3OH , the fluorescence spectra in these two solvents are almost the same. It is due to the donor ability of CH_3OH as polar protic solvent (34). The hydrogen bond donor nature of CH_3OH seems to stabilise the excited state of the electronic transitions through solute–solvent interactions. DMSO is polar aprotic solvent, which cannot be used as a hydrogen bond donor (32). As a result, the fluorescence spectra in DMSO and CH_3OH solvents are almost the same.

The change of temperature from 298 to 77 K caused a blue shift of emission peaks (ca. 6–23 nm) in the three solutions of compound **1** (Figure 5). Low- and high-energy emission bands of compound **1** are at ca. 469–477 and 421–444 nm, from CH_3CN to DMSO, respectively, and

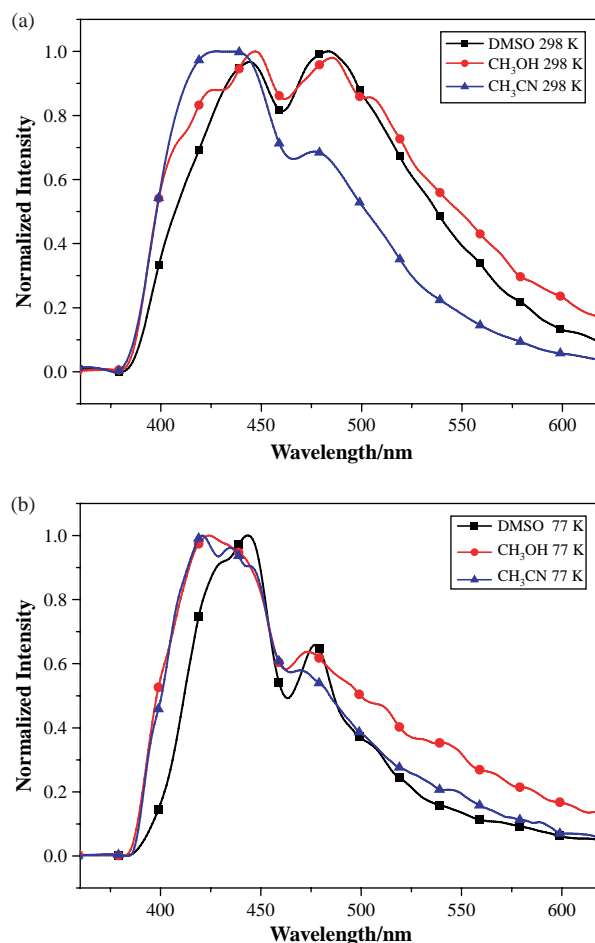


Figure 4. Normalised emission spectra of compound **1** in DMSO, CH_3OH and CH_3CN solutions (concentration: $(M) \approx 10^{-5}$ M) at (a) 298 K and (b) 77 K.

the low-energy emission bands appear as shoulders. We consider the blue shift on the change of the emitting state is closely related to vibrational coupling. At low temperature, the vibrations are hardly restricted by the interaction of energy level (35), in that case, energy of the transition from excited to ground state increase.

3.4.3. Fluorescence quantum yield and time-resolved fluorescence decay

The fluorescence quantum yields (Φ_f) of **1** were determined in DMSO, CH_3CN and CH_3OH using diluted solution (1.0×10^{-5} mol/L). Quinine sulphate with known quantum yield acts as reference fluorophore. The expression $\Phi_u/\Phi_s = F_u/F_s A_s/A_u n_u^2/n_s^2$ was used for calculating the quantum yields, in which the indices u and s refer to the sample of the compound (with unknown quantum yield) and the reference fluorophore, F is the area under the fluorescent emission curves, A denotes the absorbance at the wavelength of excitation and n is

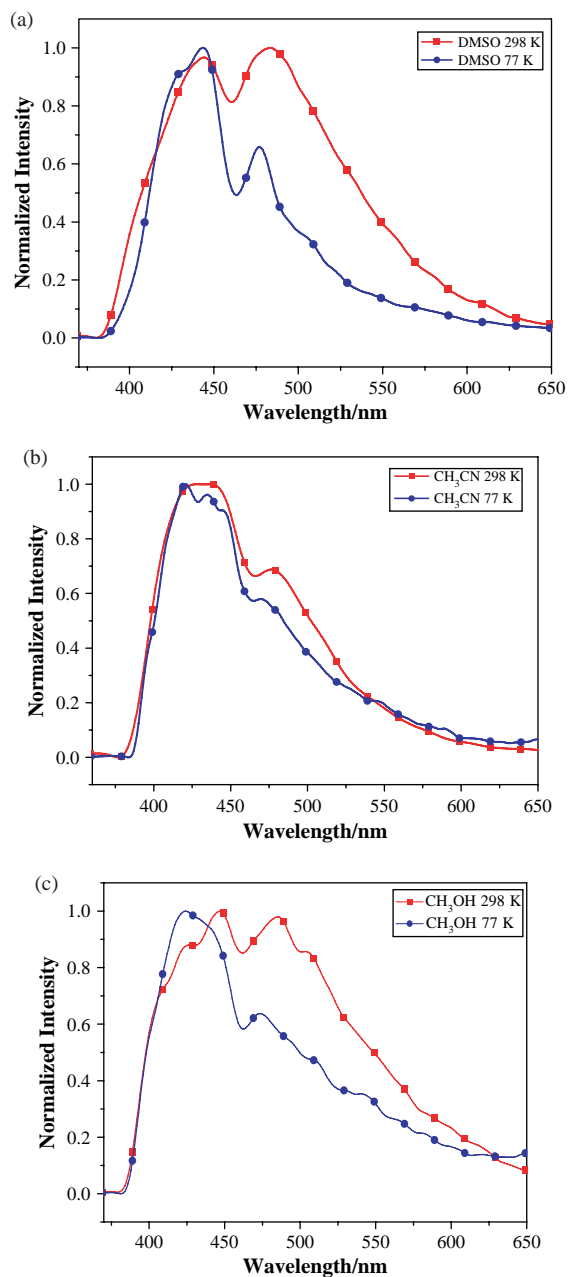


Figure 5. Normalised emission spectra of compound **1** at 298 K compared with it at 77 K in DMSO, CH₃OH and CH₃CN solutions (concentration: (M) $\approx 10^{-5}$ M).

the refractive index of the solvent (36). The value of the quantum yields for compound **1** in DMSO, CH₃CN and CH₃OH is 0.079, 0.012 and 0.166, respectively, which depends strongly on solvent properties. The remarkable increase in quantum yield (Φ_f) in polar protic solvent (CH₃OH) is observed than that in polar aprotic medium (DMSO, CH₃CN). This may be due to differential contribution of hydrogen bonding interactions.

The fluorescence lifetimes in solution (DMSO, CH₃CN and CH₃OH) of compound **1** were measured at

298 and 77 K, it showed that the lifetimes of compound **1** in solution not depend strongly on the temperature but on solution (Figure 6), corresponding data are given in Table 3. The fluorescence lifetime in DMSO at 298 K is the longest one, $\tau_1 = 0.92 \mu\text{s}$ (81.28%), $\tau_2 = 8.71 \mu\text{s}$ (18.72%). Although in CH₃OH, the fluorescence lifetime is substantially shortened comparison with that in aprotic solvents (DMSO and CH₃CN). This can be attributed to hydrogen bonding interaction in excited state of compound **1**, which enhances the non-radiative deactivation of the excited state (37).

3.5. Fluorescence spectra of **1** in solid state

The emission band for compound **1** is located at 546 nm, exhibiting strong green fluorescence in solid state at 298 K ($\lambda_{\text{ex}} = 338 \text{ nm}$) (Figure 7). In the same condition, discrete H₄OTBA molecule displays a broad peak at 481 nm ($\lambda_{\text{ex}} = 320 \text{ nm}$) (Figure 7). In contrast to H₄OTBA and in solutions, the emission band of compound **1** in solid state is red shift, which may be due to the intermolecular hydrogen bonds. The hydrogen bonds can effectively decrease the HOMO–LUMO energy gap, so as to

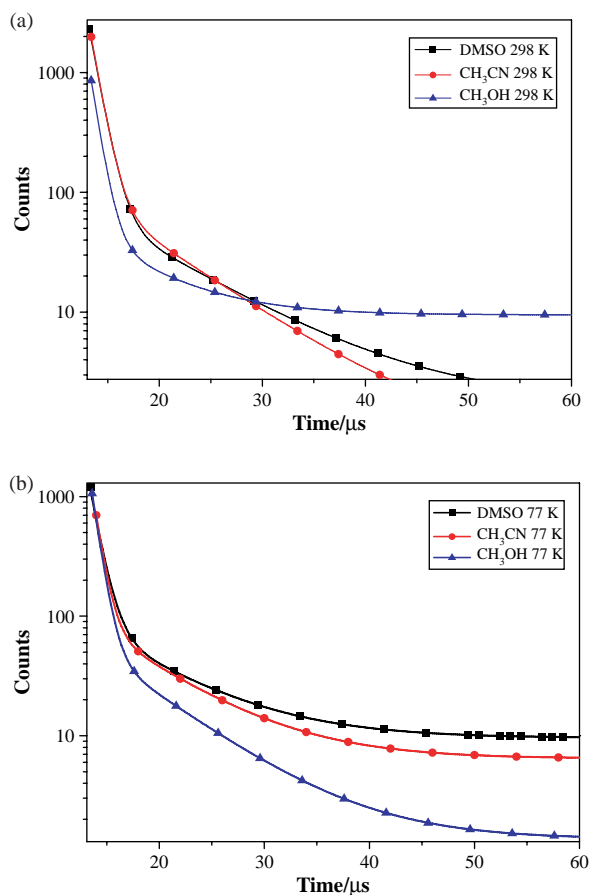


Figure 6. The decay curves of compound **1** measured in DMSO, CH₃OH and CH₃CN solutions at (a) 298 K and (b) 77 K.

Table 3. Photoluminescent data for compound **1** and H₄OTBA.

Compound	Absorption (nm) $\epsilon/\text{dm}^3\text{cm}^{-1}\text{mol}^{-1}$	Excitation (λ , nm)	Emission (λ_{max} , nm)	Lifetime (μs)	Quantum yields (Φ) ^a	Conditions ^b
1	269	291	444, 483	$\tau_1 = 0.92$ (81.28%) $\tau_2 = 8.71$ (18.72%)	0.079	DMSO, 298 K
	–	289	444, 477 ^{sh}	$\tau_1 = 0.90$ (68.89%) $\tau_2 = 7.45$ (31.11%)	–	DMSO, 77 K
	243	285	447, 485	$\tau_1 = 0.79$ (78.64%) $\tau_2 = 6.34$ (21.36%)	0.166	CH ₃ OH, 298 K
	–	324	424, 473 ^{sh}	$\tau_1 = 0.72$ (72.17%) $\tau_2 = 6.88$ (27.83%)	–	CH ₃ OH, 77 K
	229	281	428, 476 ^{sh}	$\tau_1 = 0.87$ (75.57%) $\tau_2 = 7.50$ (24.43%)	0.012	CH ₃ CN, 298 K
	–	283	421, 469 ^{sh}	$\tau_1 = 0.73$ (52.80%) $\tau_2 = 7.03$ (47.20%)	–	CH ₃ CN, 77 K
	–	338	546	$\tau_1 = 1.13$ (44.03%) $\tau_2 = 7.50$ (55.97%)	–	Solid state, 298 K
	–	316	404	$\tau_1 = 0.97$ (65.05%) $\tau_2 = 8.97$ (34.95%)	–	Solid state, 77 K
H ₄ OTBA	–	320	487	$\tau_1 = 1.05$ (54.18%) $\tau_2 = 5.56$ (45.82%)	–	Solid state, 298 K

^a Determined using quinine sulphate in 0.1 M sulphuric acid ($(M) = 1 \times 10^{-4}$ M, $\Phi_s = 0.546$).

^b Concentration in DMSO, CH₃CN and CH₃OH solution: $(M) = 1 \times 10^{-5}$ M.

influence the $\pi^* \rightarrow \pi$ transitions (38). The luminescent lifetime for compound **1** in solid state is determined to be: $\tau_1 = 1.13 \mu\text{s}$ (44.03%), $\tau_2 = 7.50 \mu\text{s}$ (55.97%), which is longer than that in DMSO. It probably because of the less polar nature of the environment in solid state (39). At 77 K,

we can see the strong blue shift in emission spectra of compound **1** (*ca.* 142 nm) (Figure 7), and the lifetime of compound **1** decreases at 77 K [$\tau_1 = 0.97 \mu\text{s}$ (65.05%), $\tau_2 = 8.97 \mu\text{s}$ (34.95%)]. It is due to the radiative rate increases and the non-radiative rate decreases for compound **1** in solid state at low temperature (40).

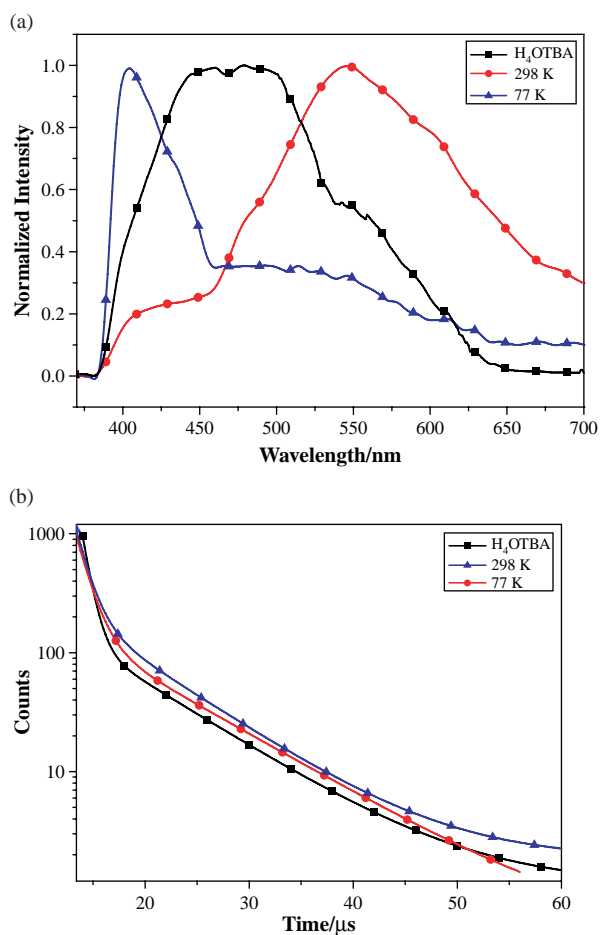


Figure 7. Normalised emission spectra (a) and decay curves (b) of H₄OTBA at 298 K and those of compound **1** at 298 and 77 K in solid state.

4. Conclusion

The supramolecular compound **1** was successfully synthesised under hydrothermal methods and its single crystal structure was confirmed by X-ray diffraction analysis. In crystal structure, significant non-covalent interactions are noted, involving O–H···O, O–H···N and π – π stacking (π – π stacking distance is 3.282 Å), on account of which a three-dimensional feature was formed. At 298 K, compound **1** exhibits an intense green fluorescent emission at 546 nm ($\lambda_{\text{ex}} = 338$ nm) in solid state. Good fluorescent properties of compound **1** reveal that it is a good fluorescence material candidate and has potential applications in optical devices. In addition, we found that the peak position of compound **1** is sensitive to the polarity of the medium as well as specific solute–solvent interaction such as hydrogen bonding. It exhibits blue–purple fluorescent emissions from DMSO, CH₃OH to CH₃CN solution at 298 K, and the UV–vis spectra show a large red shift, as the solvent polarity increases, the maximum shift was 40 nm. Moreover, the fluorescence quantum yield and lifetime of compound **1** are dependent on the polarity of the solvent. On changing temperature from 298 to 77 K, certain extent of changes occur in fluorescence spectra of compound **1** in both solution and solid state, the maximum shift is 23 and 142 nm towards blue, respectively.

Acknowledgements

This work was supported by the National Natural Science Foundation of China (Grant Nos 21071035 and 21171044), National Key Basic Research Program of China (973 Program,

No. 2013CB632900) and the Key Natural Science Foundation of Heilongjiang Province, China (No. ZD201009).

References

- (1) Desiraju, G.R. *Nature* **2001**, *412*, 397–400.
- (2) Srivastava, P.C.; Bajpai, S.; Lath, R.; Kumar, R.; Singh, V.; Dwivedi, S.; Butcher, R.J.; Hayashi, S.; Nakanishi, W. *Polyhedron* **2008**, *27*, 835–848.
- (3) Holger, G.; Gerhard, K. *Angew. Chem. Int. Ed.* **2002**, *41*, 48–76.
- (4) Müller-Dethlefs, K.; Hobza, P. *Chem. Rev.* **2000**, *100*, 143–167.
- (5) Stanley, N.; Muthiah, P.T.; Geib, S.J.; Luger, P.; Weber, M.; Messerschmidt, M. *Tetrahedron* **2005**, *61*, 7201–7210.
- (6) Barin, G.; Coskun, A.; Moustafa, M.G.; Fouda, M.M.G.; Stoddart, J.F. *ChemPlusChem* **2012**, *77*, 159–185.
- (7) Misra, A.; Kumar, P.; Kamalasanan, M.N.; Chandra, S. *Semiconduct. Sci. Technol.* **2006**, *21*, 35–47.
- (8) Zhang, H.J.; Sun, S.; Chen, X.D.; Li, C.; Sun, B.W. *Spectrochim. Acta, Part A* **2010**, *76*, 464–469.
- (9) Yi, X.Y.; Yin, P.Y.; Tong, L.; Gu, Z.G.; Chen, J.H.; Jin, H.G.; Li, S.S.; Gong, X.; Cai, Y.P. *Inorg. Chem. Commun.* **2011**, *14*, 247–250.
- (10) Liu, F.J.; Sun, D.; Hao, H.J.; Huang, R.B.; Zhenga, L.S. *CrystEngCommunity* **2012**, *14*, 379–382.
- (11) Lee, T.; Liu, Z.X.; Lee, H.L. *Cryst. Growth Des.* **2011**, *11*, 4146–4154.
- (12) Wojciechowska, A.; Kochel, A.; Komarowska, M. *Polyhedron* **2011**, *30*, 2361–2367.
- (13) Erer, H.; Yesilel, O.Z.; Darcan, C.; Büyükgüngör, O. *Polyhedron* **2011**, *30*, 2406–2413.
- (14) Ma, L.F.; Li, C.P.; Wang, L.Y.; Du, M. *Cryst. Growth Des.* **2010**, *10*, 2641–2649.
- (15) Rajesh Kumar, P.C.; Ravindrachary, V.; Janardhana, K.; Poojary, B. *J. Cryst. Growth.* **2012**, *354*, 182–187.
- (16) Wang, L.N.; Wang, X.Q.; Zhang, G.H.; Liu, X.T.; Sun, Z.H.; Sun, G.H.; Wang, L.; Yu, W.T.; Xu, D. *J. Cryst. Growth* **2011**, *327*, 133–139.
- (17) Szulmanowicz, M.S.; Zawartka, W.; Gniewek, A.; Trzeciak, A.M. *Inorg. Chim. Acta* **2010**, *363*, 4346–4354.
- (18) Jin, S.W.; Guo, M.; Wang, D.Q. *J. Mol. Struct.* **2012**, *1022*, 220–231.
- (19) Nagarapu, L.; Apuri, S.; Kantevari, S. *J. Mol. Catal. A: Chem.* **2007**, *266*, 104–108.
- (20) Wang, Y.; Zhao, Y.H.; Che, Y.X.; Zheng, J.M. *Inorg. Chem. Commun.* **2012**, *17*, 180–183.
- (21) Geng, W.Q.; Zhou, H.P.; Cheng, L.H.; Hao, F.Y.; Xu, G.Y.; Zhou, F.X.; Yu, Z.P.; Zheng, Z.; Wang, J.Q.; Wu, J.Y.; Tian, Y.P. *Polyhedron* **2012**, *31*, 738–747.
- (22) Li, F.; Zhu, Y.C.; You, B.; Zhao, D.H.; Ruan, Q.C.; Zeng, Y.; Ding, C.X. *Adv. Funct. Mater.* **2010**, *20*, 669–676.
- (23) Dong, S.Q.; Tian, H.K.; Huang, L.Z.; Zhang, J.D.; Yan, D.H.; Geng, Y.H.; Wang, F.S. *Adv. Mater.* **2011**, *23*, 2850–2854.
- (24) Sheldrick, G.M. *SHELXTL NT Crystal Structure Analysis Package, Version 5.10*; Bruker Axs, Analytical X-Ray System: Madison, WI, 1999.
- (25) Lin, Z.Z.; Jiang, F.L.; Chen, L.; Yuan, D.Q.; Hong, M.C. *Inorg. Chem.* **2005**, *44*, 73–76.
- (26) Han, Z.B.; Song, Y.J.; Ji, J.W.; Zhang, W.; Han, G.X. *J. Solid State Chem.* **2009**, *182*, 3067–3070.
- (27) Kosar, B.; Albayrak, C.; Ersanlı, C.C.; Odabasoglu, M.; Büyükgüngör, O. *Spectrochim. Acta, Part A* **2012**, *93*, 1–9.
- (28) Hammud, H.H.; Ghannoum, A.; Masoud, M.S. *Spectrochim. Acta, Part A* **2006**, *63*, 255–265.
- (29) Zhou, Y.X.; Shen, X.Q.; Du, C.X.; Wu, B.L.; Zhang, H.Y. *Eur. J. Inorg. Chem.* **2008**, *27*, 4280–4289.
- (30) Liu, L.S.; Sun, Y.; Wei, S.; Hu, X.Y.; Zhao, Y.Y.; Fan, J. *J. Spectrochim. Acta, Part A* **2012**, *86*, 120–123.
- (31) Sowmiya, M.; Tiwari, A.K.; Sonu Saha, S.K. *J. Photochem. Photobiol. A* **2011**, *218*, 76–86.
- (32) Fisli, H.; Bensouilah, N.; Dhaoui, N.; Abdaoui, M. *J. Inc. Phenom. Macrocyc. Chem.* **2012**, *73*, 369–376.
- (33) Fu, Y.M.; Zhao, Y.H.; Lan, Y.Q.; Shao, K.Z.; Qiu, Y.Q.; Hao, X.R.; Su, Z.M. *J. Solid State Chem.* **2008**, *181*, 2378–2385.
- (34) Moyon, N.S.; Chandra, A.K.; Mitra, S. *J. Phys. Chem. A* **2010**, *114*, 60–67.
- (35) Ivanov, P.; Stanimirov, S.; Kaloyanova, S.; Petkov, I. *J. Fluoresc.* **2012**, *22*, 1501–1507.
- (36) Kubinyi, M.; Varga, O.; Baranyai, P.; Kállay, M.; Mizsei, R.; Tárkányi, G.; Vidóczy, T. *J. Mol. Struct.* **2011**, *1000*, 77–84.
- (37) Asiri, A.M.; El-Daly, S.A.; Khan, S.A. *Spectrochim. Acta, Part A* **2012**, *95*, 679–684.
- (38) Fan, R.Q.; Zhang, Y.J.; Yin, Y.B.; Su, Q.; Yang, Y.L.; Hasi, W. *Synth. Met.* **2009**, *159*, 1106–1111.
- (39) Murugan, K.D.; Natarajan, P. *Eur. Polym. J.* **2011**, *47*, 1664–1675.
- (40) Dijken, A.V.; Meulenkamp, E.A.; Vanmaekelbergh, D.; Meijerink, A. *J. Phys. Chem. B* **2000**, *104*, 1715–1723.